

Topics in coarsening phenomena

in Fundamental Problems in Statistical Physics XII Leuven, Aug 30 - Sept 12, 2009

Leticia F. Cugliandolo
Université Pierre et Marie Curie - Paris VI
Laboratoire de Physique Théorique et Hautes Energies

October 26, 2018

Abstract

These lecture notes give a very short introduction to coarsening phenomena and summarize some recent results in the field. They focus on three aspects: the super-universality hypothesis, the geometry of growing structures, and coarsening in the spiral kinetically constrained model.

1 Introduction

These notes are complementary to my lectures at FPSP XII. My aim is to discuss in this text some recent developments in the theory of coarsening phenomena [1] (although I only covered some of them in the talks). Coarsening is possibly the simplest example of macroscopic non-equilibrium relaxation and it has very far-reaching practical applications. This problem, although pretty old and rather well understood qualitatively, is still far from having a close and satisfactory quantitative description going beyond the pretty successful but somehow deceiving use of the dynamic scaling hypothesis.

After presenting the models I shall focus on and the coarsening phenomenon, I shall discuss the following aspects: (1) super-universality; (2) the statistics and geometry of evolving ordered structures; (3) domain growth in a kinetically constrained spin model, the two dimensional spiral model. Some reasons why we studied these problems are the following. We wished to check the super-universality hypothesis in more detail than what it had been done so far. In our opinion, establishing the validity of this hypothesis might be useful to eventually develop a successful analytic method to compute scaling functions in coarsening problems. We analyzed the geometry of domain growth with similar ideas to the ones used in the study of critical equilibrium structures in the past. Knowing in detail the time-dependent distribution of structures and their geometric

properties might give us hints into what to search for in more complex systems with out of equilibrium dynamics such as glasses. In this respect, kinetically constrained models are supposed to be toy models for glassy relaxation. We demonstrated that the mechanism of relaxation in the spiral model is of the coarsening type. This is interesting *per se* and for applications to glassy physics too. In short, apart from making our understanding of coarsening more complete, we expect that these results might be useful to better grasp the more complex dynamics of glassy systems.

References to the original articles will be given in the main text. My results on this field have been obtained in collaboration with the colleagues and students that I warmly thank in the acknowledgements.

2 Models

In this section we introduce three kinds of problems with phase transitions: purely geometric models with percolation as the standard example; models with an energy (or cost) function that have both static and dynamic transitions, with Ising and Potts spin models as typical instances; and models with purely dynamic phase transition such as kinetically constrained spin systems focusing on the bi-dimensional spiral model. Related to the latter case, I shall also mention coupled map lattices as well as spin models with dynamic rules that do not satisfy detailed balance.

2.1 Geometric and probabilistic models

We recall the definition of two purely geometric and probabilistic models: site and directed percolation. These models change behaviour at a special value of their control parameter, p_c , and this threshold has many points in common with usual thermal second-order phase transitions. Percolation theory deals mainly with the critical phenomenon and the study of cluster sizes and their geometric properties.

2.1.1 Site percolation

Percolation is the propagation of activities through connected space. The site percolation model [2] is defined as follows. For each site on the considered lattice one tosses a coin independently. With probability p the site is occupied and with probability $1 - p$ it remains empty. A configuration is constructed by sweeping the lattice once and filling the sites (or not) independently with this rule.

Clusters are defined as groups of first-neighbour filled (or empty) sites. At a (lattice dependent) threshold p_c an infinite cluster (on an infinite lattice) appears. Strictly speaking, for $p \leq p_c$ ($1 - p \leq p_c$) there is no infinite connected-component of filled (empty) sites with probability one while for $p > p_c$ ($1 -$

$p > p_c$) there is an infinite connected-component of filled (empty) sites with probability one. The critical values of p_c in some typical bi-dimensional lattices are: $p_c = 1/2$ (triangular), $p_c \approx 0.59$ (square), $p_c \approx 0.62$ (honeycomb).

Percolation can be obtained as a limit of the Potts model (see its definition below) with $q \rightarrow 1$ [5].

2.1.2 Directed percolation

Directed percolation [3] is percolation with a special direction along which the activity propagates. It mimics filtering of fluids through porous materials along a given direction. For example, in the percolation of coffee making, the source is the top surface of the grounded coffee that receives the water and the activity is to have water flow. On a square lattice the model is defined by assigning a directed bond on horizontal (say, pointing to the left) and vertical (say, pointing down) edges with probability p . This mimics different microscopic pore connectivity. This model displays a phase transition from a macroscopically permeable (percolating) to an impermeable (non-percolating) state. Directed percolation on a $2d$ square lattice has a transition at $p_c \simeq 0.705$.

More generally, the terms percolation and directed percolation stand for universality classes of continuous phase transitions which are characterized by the same type of collective behavior on large scales. A number of critical exponents, linked to the size of the percolation cluster, correlation functions, and so on can be defined similarly to what is done in thermal critical phenomena [2].

2.2 Hamiltonian systems

Physical models, as well as some mathematical problems such as those requiring optimisation, have an energy or cost function associated to each configuration. In equilibrium, the configurations are sampled with a probability distribution function that depends on their energy and the external parameters such as temperature or a chemical potential. The experimental conditions, that is to say whether the system is isolated or in contact with thermal or particle reservoirs, dictate the statistical ensemble to be used (micro-canonical, canonical or gran-canonical). Out of equilibrium, say when the system is let evolve from an initial condition that is not one selected from the equilibrium measure, the system wanders in phase space in a manner that we shall discuss below.

2.2.1 The Ising model

Anisotropic magnets are modeled in a very simple way by using Ising spins, $s_i = \pm 1$, to describe the magnetic moments and by choosing an adequate interaction among them. The Hamiltonian of the d dimensional Ising model is

$$H = - \sum_{\langle ij \rangle} J_{ij} s_i s_j . \quad (1)$$

The spin variables are placed on the vertexes of a lattice and the sum runs over nearest-neighbours. The exchange interactions J_{ij} are all positive, favouring ferromagnetism but they can, in principle, take different values. We shall focus on the usual uniform case $J_{ij} = J$, that is to say the clean model, and the case in which the J_{ij} 's are quenched random variables drawn from a probability distribution with positive support, a dirty case. The latter defines the random-bond Ising model (RBIM). One can also add a random field term to the uniform model and thus construct the random field Ising model (RFIM).

A totally random spin configuration in which $s_i = \pm 1$ with probability a half is a realization of a site percolation configuration with $p = 1/2$ and, in $d = 2$, neither positive nor negative clusters percolate. The identification is achieved by defining site occupation variables $n_i = (s_i + 1)/2 = 0, 1$.

The static properties of the Ising model (1) are more easily analyzed in the experimentally relevant canonical ensemble in which the system is coupled to a thermal reservoir at temperature T . A second-order continuous phase transition at a finite critical temperature, T_c , separates a high-temperature disordered paramagnetic phase from a low-temperature ferromagnetic ordered one. see Fig. 1. T_c depends on d and the statistics of the interaction strength. The nature of the two phases is understood since the development of the Curie-Weiss mean-field theory while the critical phenomenon has been accurately described with the help of the renormalization group, that allows for the computation of all critical exponents [4].

2.2.2 The Potts model

A natural generalization of the Ising model is the Potts model [5] in which the spins σ_i take q integer values from 1 to q . The Hamiltonian is given by

$$\mathcal{H} = - \sum_{\langle ij \rangle} J_{ij} \delta_{\sigma_i \sigma_j} \quad (2)$$

where the sum is over nearest-neighbours on the lattice. Either uniform, $J_{ij} = J$ (pure case), or bimodal $P(J_{ij}) = p\delta(J_{ij} - J_1) + (1-p)\delta(J_{ij} - J_2)$ (random case) interactions are usually studied. In $d = 2$ the transition, discontinuous for $q > 4$ and continuous for $q \leq 4$, occurs at $(e^{\beta_c J_1} - 1)(e^{\beta_c J_2} - 1) = q$ in the random case with $p = 1/2$. T_c for the pure limit is recovered by setting $J_1 = J_2$.

Soap films and general grain growth [6] are two physical systems mimicked by Potts models. In $2d$ these physical systems are made of polygonal-like cells separated by thin walls endowed with line energy; different 'colour' domains correspond to different cells.

2.3 Microscopic dynamics

Once the Hamiltonians have been defined, we need to assign updating rules to the microscopic variables. Classically, the spins do not have an intrinsic

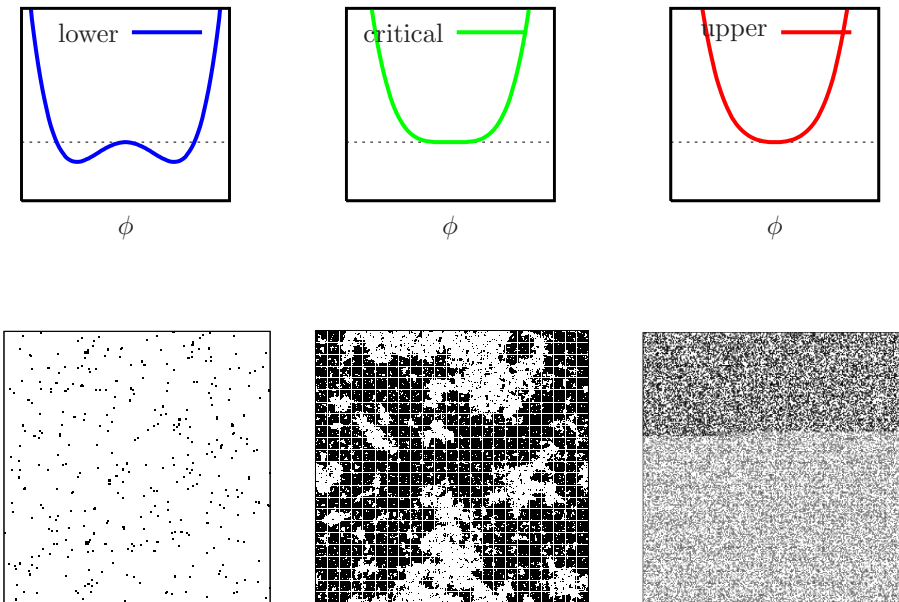


Figure 1: An equilibrium free-energy landscape with a second-order phase transition between two phases, a single-valued one with one minimum, and a bi-valued one with minima related by parity. Below are three snapshots of a spontaneously broken state at $g < g_c$, a critical configuration at $g = g_c$, and a disordered one at $g > g_c$, in the $2dIM$. Black and white dots represent up and down spins, respectively.

dynamics. Quite generally, we are interested in the evolution of physical systems in contact with an environment that provides thermal agitation and dissipation. Thus, the evolution is assumed to be stochastic [7] and it does not conserve the total energy. If we want to let the system reach equilibrium at sufficiently long times we use dynamic rules that satisfy detailed balance:

$$W(C \rightarrow C')P_{eq}(C) = W(C' \rightarrow C)P_{eq}(C'), \quad (3)$$

with $W(C \rightarrow C')$ the transition probability from configuration C to configuration C' and $P_{eq}(C) = e^{-\beta H(C)} / \sum_{C''} e^{-\beta H(C'')}$ the Boltzmann weight. Finally, one has to decide whether there are conserved quantities, for instance the global magnetization, $M = \sum_{i=1}^N s_i$, or a local one, *e.g.* $m_{loc} = s_i + s_j$ with i and j nearest-neighbours. The existence of conserved quantities puts constraints on the microscopic updates. In the context of Ising and Potts models two types of dynamics are common:

Non-conserved order parameter; there are no constraints on the stochastic moves

and two examples are Monte Carlo or Glauber dynamics for Ising spins [8]. *Conserved order parameter*; it mimics particle-hole exchanges in lattice gas models obtained from a mapping of the Ising model and the local magnetization is conserved. Exchanges of up and down spins are proposed and these are accepted with a probabilistic law (Kawasaki dynamics [8]). *Kinetic constraints* Spin updates are allowed (and realized with some stochastic rule) only when a chosen constraint is satisfied, typically by neighbor variables.

Dynamical systems are defined by dynamic rules that do not necessarily satisfy detail balance and have no reference to any equilibrium energy (or free-energy) that they should minimize. Up to what extent the stochastic and deterministic evolution of some macroscopic systems are similar or even equivalent at some length and time scales is a relevant question. Some issues one would like to understand are under which conditions collective behaviour emerges in extended dynamical systems with short-range interactions and local chaotic dynamics; and whether thermodynamic and statistical mechanics concepts apply in some dynamic regimes, in particular, whether an energy function and a temperature can be identified in deterministic dissipative systems. In spatially extended dynamical systems the effective noise strength, that may play the role of temperature, is internally generated rather than imposed by an environment. Some lattice models of coupled chaotic maps present dynamic phase transitions between dynamic phases that can be associated to a disorder state and a bi-valued dynamically ordered one by using a spin representation. This is the case of the Miller-Huse coupled map lattice [9], for example, the transition of which presents many similarities with critical phenomena.

Problems that originate in other sciences, suchlike social studies, informatics, *etc.* can sometimes be formulated by using stochastic dynamic rules that do not satisfy detail balance. In some cases, collective behaviour gives rise to dynamic phase transitions between phases [3] and by choosing adequately the dynamic rules one may also encounter a dynamic transition similar to the ones mentioned above. This is the case, for instance, of some variants of *voter models* [10].

2.4 The spiral model

Spin kinetically constrained models capture many features of real glass-forming systems (see [11] for reviews). These models display no thermodynamic singularity: their equilibrium measure is simply the Boltzmann factor of independent spins and correlations only reflect the hard core constraint. Bootstrap percolation arguments allowed C. Toninelli *et al.* to show that, when defined on finite dimensional lattices, these models do not even have a dynamic transition at a particle density that is less than unity in the thermodynamic limit [12]. On Bethe lattices instead a dynamical transition similar to the one predicted by the mode coupling theory might occur [13]. The quest to define a finite dimensional kinetically constrained model with a (discontinuous) transition was

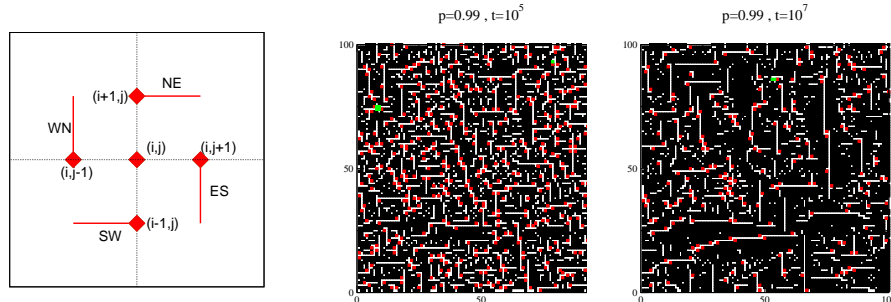


Figure 2: Left: The neighbouring sites determining the frozen or free to move character of the center site (i, j) . Centre and right panel: Configuration of the system at two times ($t = 10^5$ and $t = 10^7$) in a quench to $p = 0.99$. Black and white sites are frozen particles and vacancies, respectively. Red and green sites are particles and holes that can be updated. Figure taken from [15].

positively answered by C. Toninelli *et al* who constructed the so-called spiral model, a finite dimensional kinetically constrained model with an ideal *glass-jamming* dynamic transition at a particle density that is different from one [14]. A binary variable $n_{ij} = 0, 1$ is defined on the sites (i, j) of an $L \times L$ periodic bi-dimensional square lattice. $n_{ij} = 1$ if a particle occupies the site and $n_{ij} = 0$ otherwise. One defines the couples of neighbouring sites (see Fig. 2-left):

- $(i, j + 1), (i + 1, j + 1)$, north east (NE) couple;
- $(i + 1, j), (i + 1, j - 1)$, east south (ES) couple;
- $(i, j - 1), (i - 1, j - 1)$, south west (SW) couple;
- $(i - 1, j), (i - 1, j + 1)$, west north (WN) couple.

Whether the variable n_{ij} may be updated or not depends on the configuration on these pairs: if the sites belonging to at least two consecutive couples (namely, NE+ES or ES+SW or WN+NW or WN+NE) are empty site (i, j) can be updated (either emptied or filled). Otherwise it is blocked. Each site is coupled to a particle reservoir in such a way that particles can enter or leave the sample from its full volume. Defining $M_{ij} = 0$ if site (i, j) is frozen and $M_{ij} = 1$ otherwise the updating rule can be expressed in terms of the transition rates $W(n_{ij}|n'_{ij})$ to add or remove a particle as $W_p(0|1) = M_{ij} p$ and $W_p(1|0) = M_{ij} (1 - p)$. The model can be regarded as a two-level system described by $H = - \sum_{ij} (2n_{ij} - 1)$ at the inverse temperature $\beta = (1/2) \ln[p/(1 - p)]$. When $p \rightarrow 1/2$ the inverse temperature vanishes $\beta \rightarrow 0$ whereas for $p \rightarrow 1$ it diverges $\beta \rightarrow \infty$. The Bernoulli measure implies $\rho = \langle n_{ij} \rangle = p$ for the equilibrium density of particles. In equilibrium at zero temperature ($p \rightarrow 1$), the lattice is full while at infinite temperature ($p \rightarrow 1/2$) it is half-filled. The existence of a blocked cluster

at $p \geq p_c < 1$ was shown by studying the critical p above which an equilibrium configuration cannot be emptied and this coincides with the threshold for $2d$ directed percolation ($p_c \simeq 0.705$). At the transition an infinite cluster of blocked particles exists and the density of the frozen cluster is discontinuous at p_c . Many aspects of super-cooled liquids slowing down are reproduced close (but below) p_c [14]. In Sect. 7 we shall summarize results in [15] where we studied, in particular, the dynamics following a quench from $p_0 < p_c$ to $p > p_c$.

3 Geometric description of phase transitions

Geometric domains are ensembles of connected nearest-neighbour sites with spins pointing in the same direction. Their area is the number of spins belonging to the domain. By lumping together with a certain temperature-dependent probability neighboring spins in the same spin state, spin models can be mapped onto percolation theory. The resulting Fortuin-Kasteleyn spin clusters [16] built using $p_{ij} = 1 - e^{-\beta J_{ij}}$ percolate at the critical temperature, and their percolation exponents coincide with the thermal ones. In this way, a purely geometrical description of the phase transition is achieved. In the rest of this Section we sum up the definitions of the main geometric objects used in such a static description of critical phenomena.

3.1 Definitions

A number of linear dimensions of a cluster can be defined. The radius of gyration is

$$R_g^2 = s^{-1} \sum_{i=1}^s |\vec{r}_i - \vec{r}_{cm}|^2 \quad (4)$$

with the centre of mass position given by $\vec{r}_{cm} = s^{-1} \sum_{i=1}^s \vec{r}_i$.

Take the cluster site with the largest (smallest) y component and among these the one with the largest (smallest) x component. These sites are the two ‘end-points’ of the cluster. The end-to-end length of the cluster, ℓ , is the Euclidean distance between these two points.

There are also several ways of defining the surface of a cluster [2]. Different definitions are relevant to different applications that have to do, for example, with the adsorption of particles on the surface. Without entering into all the zoology let us recall some of these definitions.

The external border of a cluster of occupied sites is the set of vacant sites that are nearest-neighbours to sites on the cluster and are connected to the exterior by (a) nearest *and* next-to-nearest neighbours or (b) just next nearest neighbours. Figure 3 (a) and (b) show the external borders of a cluster of occupied sites thus defined. Note that in (a) there are two ‘inner’ sites that belong to the external border and that are connected to the outside by a narrow

neck of width $\sqrt{2}a$ with a the lattice spacing while in (b) these two sites do not belong to the border and the ‘fjord’ has been excluded.

The hull is the envelop of a cluster, meaning the ensemble of cluster sites obtained by using a biased walk that encircles the cluster on its left and on its right linking the lowest lying site to the left and the highest lying site to the right, see Fig. 4. The hull of a cluster of occupied (vacant) sites lies on occupied (vacant) sites.

The hull-enclosed area is the total area within the hull (including the sites on the hull). It therefore ignores the type of site (occupied or vacant, spin up or spin down) that lies within and counts them all on equal footing.

3.2 Number densities

We call $n(s)$ the number of objects (hulls, clusters, *etc.*) with s sites per unit number of lattice sites. Scaling theory, some exactly solvable cases (*e.g.* the Bethe lattice), renormalization group arguments [2], Coulomb gas mappings, conformal field theory calculations, stochastic Loewner evolution techniques [17, 18] and numerical experiments [19] suggest

$$n(s) \sim s^{-\tau} f[\theta s^\sigma] \quad \text{for large } s, \quad (5)$$

with τ and σ two control parameter and lattice-independent exponents that do depend on the space dimensionality and θ measuring the distance from criticality, say $\theta = |g - g_c|$ with g the control parameter. The function $f(z)$ approaches a constant for $|z| \ll 1$ and it falls-off rapidly for $|z| \gg 1$; it thus provides a cut-off with a *unique* cross-over size $s_\xi \equiv |g - g_c|^{-1/\sigma}$ such that clusters with $s < s_\xi$ are effectively critical while those with $s > s_\xi$ are not. At criticality ($g = g_c$) the factor $f[\theta s^\sigma] = f[0]$ that suppresses large objects is absent and clusters of all sizes are present.

The exponents σ and τ determine all critical exponents of percolation through scaling relations. As regards thermal phase transitions, once the relevant Fortuin-Kasteleyn clusters are constructed and analysed their two independent exponents σ and τ determine the entire set of thermal critical exponents (see, however, [20]).

3.3 Fractal exponents

Geometric objects at criticality have a fractal behaviour, that is to say [2]

$$s \propto \ell^D. \quad (6)$$

s is the mass of the object (cluster area, its external border, its hull), ℓ is the linear size of the cluster, say its radius of gyration, and D is the fractal dimension. The fractal dimension D is related to the exponent τ in eq. (5) via $\tau = d/D + 1$ where d is the space dimension.

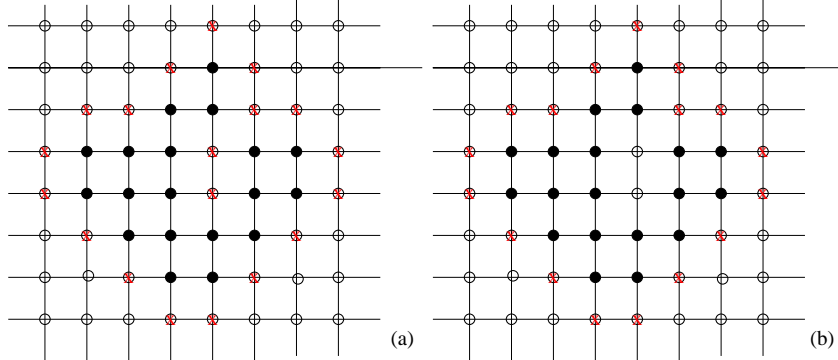


Figure 3: Square bi-dimensional lattice. Filled (empty) circles represent occupied (empty) sites. Red crosses indicate external border of the cluster of filled sites including (a), or nor (b), vacant sites that are connected to the exterior by a next nearest neighbour (a ‘diagonal’).

The fractal exponents depend strongly on the precise definition of the geometric object. For instance, Saleur and Duplantier showed that $2d$ critical percolation clusters have $D_E = 4/3$ and $D_H = 7/4$ where H stands for hull and E for external border connected to the exterior by nearest-neighbour vacant sites only [21] (case (b) in Fig. 3).

In [22] we studied the relation between areas and perimeters

$$A \propto p^\alpha \tag{7}$$

with p defined as the number of broken bonds on the external border or, equivalently, with a small variant of the Grossman-Aharony construction [2] including fjords. Note that if $A \propto \ell^{D_A}$ and $p \propto \ell^{D_p}$ with ℓ the linear size of the object, say the radius of gyration, then $\alpha = D_A/D_p$.

4 Coarsening

Take a system in equilibrium in the symmetric (positive $g - g_c$, high temperature) phase and quench it into the symmetry breaking (negative $g - g_c$, low temperature) phase through a second order phase transition. For concreteness, we focus on problems with two equilibrium states related by Z_2 symmetry. Once set into the ordered phase the system *locally* selects one (among the two possible) equilibrium configurations. However, different ‘states’ are picked up at different locations and topological defects in the form of domain walls are created. In the course of time the patches of ordered regions tend to grow while the

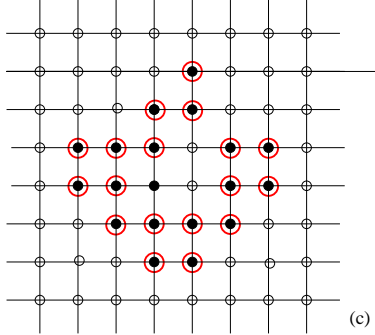


Figure 4: Same cluster as in Fig. 3. Encircled are the sites on the cluster that belong to its hull. The hull-enclosed area is everything that lies within the hull.

density of topological defects diminishes. In an infinite system this coarsening process goes on forever.

An example of the above process is given by an Ising magnet. An initial condition in equilibrium at, for instance, infinite temperature is just a random configuration in which each spin takes one of its possible values with probability $1/2$. After a quench below the critical temperature, $T < T_c$, the ferromagnetic interactions tend to align the neighbouring spins in ‘parallel’ direction (same value of the spin) and in the course of time domains of the ordered phases form and grow. At any finite time the configuration is such that both types of domain exist. Under more careful examination one reckons that there are some spins reversed within the domains. These ‘errors’ are due to thermal fluctuations and are responsible of the fact that the magnetization of a given configuration within the domains is smaller than one and close to the equilibrium value at the working temperature (apart from fluctuations due to the finite size of the domains). At each instant there are as many spins of each type (up to fluctuating time-dependent corrections that vanish in the infinite size limit). As time passes the typical size of the domains increases in a way that we shall discuss below.

Coarsening from an initial condition that is not correlated with the equilibrium state and with no bias field does not take the system to equilibrium in finite times with respect to a function of the system’s linear size, L . More explicitly, if the growth law is a power law [see eq. (10)] one needs times of the order of L^{z_d} to grow a domain of the size of the system. This gives a rough estimate of the time needed to take the system to one of the two equilibrium states. For any shorter time, domains of the two types exist and the system is out of equilibrium.

We thus wish to distinguish the relaxation time, t_r , defined as the time needed for a given initial condition to reach equilibrium with the environment,

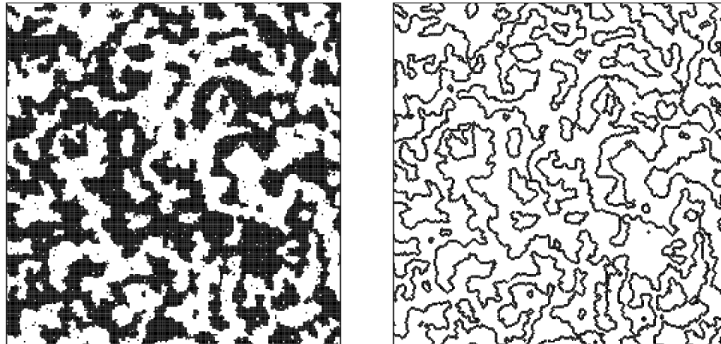


Figure 5: Snapshot of the $2d$ Ising model at a number of Monte Carlo steps after a quench from infinite to a sub-critical temperature. Left: the up and down spins on the square lattice are represented with black and white sites. Right: the domain walls are shown in black. Figure taken from [22].

from the decorrelation time, t_d , defined as the time needed for a given configuration to decorrelate from itself. At $T < T_c$ the relaxation time of *any* initial condition that is not correlated with the equilibrium state diverges with the linear size of the system. The self-correlation of such an initial state evolving at $T < T_c$ decays as a power law and although one cannot associate to it a decay time as one does to an exponential, one can still define a characteristic time that turns out to be related to the age of the system.

In contrast, the relaxation time of an *equilibrium* magnetized configuration at temperature T vanishes since the system is already in equilibrium while the decorrelation time is finite and given by $t_d \sim |T - T_c|^{-\nu z_{eq}}$.

The lesson to learn from this comparison is that the relaxation time and the decorrelation time not only depend on the working temperature but they also depend strongly on the initial condition. Moreover, the relaxation time depends on (N, T) while the decorrelation time depends on (T, t_w) . For a random initial condition one has

$$t_r \simeq \begin{cases} \text{finite} & T > T_c, \\ |T - T_c|^{-\nu z_{eq}} & T \gtrsim T_c, \\ L^{z_d} & T < T_c. \end{cases}$$

4.1 Critical coarsening

Right after a quench to the critical point the system starts to evolve out of equilibrium towards a target equilibrium configuration of the kind shown in the

central snapshot in Fig. 1. The non-equilibrium relaxation shows coarsening features with the growth of ordered structures with a typical linear length given by $R_c(t) \simeq t^{1/z_{eq}}$, and features of equilibrium dynamics, as the fact that z_{eq} is the equilibrium dynamics exponent. Interestingly enough, the early relaxation exhibits universal scaling properties characterized by usual static exponents as well as the dynamic one. This and other details of the critical equilibrium and out of equilibrium dynamics can be computed with renormalization group techniques [23, 24].

4.2 Dynamic scaling hypothesis

The dynamic scaling hypothesis states that at late times and in the scaling limit [1]

$$r \gg \xi(g), \quad R(g, t) \gg \xi(g), \quad r/R(g, t) \text{ arbitrary}, \quad (8)$$

where r is the distance between two points in the sample, $r \equiv |\vec{x} - \vec{x}'|$, and $\xi(g)$ is the equilibrium correlation length that depends on all parameters (T and possibly others) collected in g , there exists a single characteristic length, $R(g, t)$, such that the domain structure is, in statistical sense, independent of time when lengths are scaled by $R(g, t)$. Time, denoted by t , is typically measured from the instant when the critical point is crossed. In the following we ease the notation and write only the time-dependence in R . This hypothesis has been proved analytically in very simple models only, such as the one dimensional Ising chain with Glauber dynamics or the Langevin dynamics of the d -dimensional $O(N)$ model in the large N limit. In the vast majority of coarsening systems the dynamic scaling hypothesis applies. Still, a few counter-examples where two lengths grow in competition are also known [1].

In practice, the dynamic scaling hypothesis implies that the real-space correlation function should behave as

$$C(r, t) \equiv \langle s_i s_j \rangle_{|\vec{r}_i - \vec{r}_j| = r} \simeq F[r/R(t)]. \quad (9)$$

See Fig. 6 for a test of the scaling hypothesis in the MC dynamics of the $2d$ Ising and Potts model (see the caption for details). In order to fully characterise the correlation functions one then has to determine the typical growing length, R , and the scaling functions, f_c , F , *etc.*

4.2.1 The growing length

It turns out that R can be determined with semi-analytic arguments and the predictions are well verified numerically – at least for clean system. In pure and isotropic systems the growth law is

$$R(t) = \lambda t^{1/z_d} \quad (10)$$

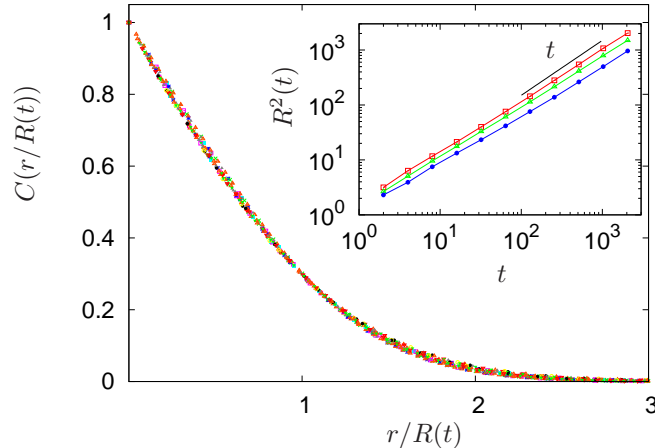


Figure 6: Check of dynamic (super-)scaling in the space-time correlation of the Potts model quenched from $T_0 \rightarrow \infty$ to $T_f = T_c(q)/2$. Data taken at several times (from $t = 2^4$ MCs to 2^{11} MCs) for $q = 2, 3$ and 8 , with and without weak disorder are shown. Distance is rescaled by the $R(t)$ obtained from $C(R, t) = 0.3$. Inset: $R^2(t)$ against t in a double logarithmic scale for $q = 2, 3$ and 8 (from top to bottom). The characteristic length, related to the average domain radius, depends weakly on q and T for the pure model (through the pre-factor). Within the time window explored there are still some small deviations from the $R(t) \simeq t^{1/2}$ expected law in the case $q = 8$. When weak disorder is introduced (not shown), the growth rate is greatly reduced and deviates from the linear behavior, see Sect. 5.2. Figure taken from [25].

with z_d the dynamic exponent (see [1]) and λ a material/model dependent prefactor that weakly depends on temperature and other parameters. In curvature driven Ising or Potts cases with non-conserved order parameter the domain walls have finite width and $z_d = 2$. For systems with continuous variables such as rotors or XY models and non-conserved order-parameter dynamics, a number of computer simulations have shown that domain walls are thicker and $z_d = 4$. The effects of temperature enter only in the parameter λ and, for clean systems of Ising type, growth is slowed down by temperature since thermal fluctuation tend to roughen the interfaces thus opposing the curvature driven mechanism. Let us list some special cases below and sketch how z_d can be estimated.

Clean one dimensional cases with non-conserved order parameter

In one dimension, a space-time graph allows one to view coarsening as the diffusion and annihilation upon collision of point-like particles that represent the domain walls. In the Glauber Ising chain with non-conserved dynamics one finds that the typical domain length grows as $t^{1/2}$ while in the continuous case

the growth is only logarithmic, $\ln t$.

Non-conserved curvature driven dynamics ($d > 2$)

The time-dependent Ginzburg-Landau model allows us to gain some insight on the mechanism driving the domain growth and the direct computation of the averaged domain length. This is a stochastic partial differential equation on a coarse-grained order parameter field with a deterministic force that is phenomenologically proposed to derive from a Ginzburg-Landau type free-energy. In clean systems temperature does not play a very important role in the domain-growth process, it just adds some thermal fluctuations within the domains, as long as it is smaller than T_c . In dirty cases instead temperature triggers thermal activation.

We focus first on zero temperature clean cases with Ising-like symmetry. At $T = 0$ the GL equation is just a gradient descent in a (free-)energy landscape, F . Two terms contribute to F : an elastic energy $(\nabla\phi)^2$ which is minimized by flat walls if present and a bulk-energy term that is minimized by constant field configurations, say $\phi = \pm\phi_0$ in an Ising-like case. If the walls are sharp enough, that is to say their width remains finite when the distance between them diverges, interface-interface interactions can be neglected and the minimization process implies that regions of constant field grow and get separated by flatter and flatter walls. Within this scenario one can easily derive the Allen-Cahn equation [26] that states that the local wall velocity is proportional to the local geodesic curvature and is normal to the wall pointing in the direction of reducing curvature:

$$\vec{v} \equiv \partial_t \hat{n}|_\phi = -\vec{\nabla} \cdot \hat{n} \hat{n} \equiv -\frac{\lambda}{2\pi} \kappa \hat{n}, \quad (11)$$

in all d . This equation yields an intuition on the typical growth law in such processes. Take a spherical wall in any dimension. The local curvature is $\kappa = (d-1)/R$ where R is the radius of the sphere within the wall. Equation (11) is recast as $dR/dt = -\lambda(d-1)/R$ that implies $R^2(t) = R^2(0) - 2\lambda(d-1)t$ and R decreases as $t^{1/2}$. This calculation implies that all hull-enclosed areas decrease in time with the same law, independently of their own size and of all others. Interestingly enough, similar results are obtained for the area loss of a square domain embedded in a sea of the opposite sign using Monte Carlo or Glauber dynamics at zero temperature for a system defined on a square lattice [27].

The above results do not imply that all domains shrink as well since some gain size from the disappearance of inner objects. Temperature effects are simply taken into account by a material and T -dependent proportionality constant λ in the Allen-Cahn equation.

In $d = 2$ the time dependence of the area contained within any finite hull on a flat surface is derived by integrating the velocity around the envelope and using the Gauss-Bonnet theorem:

$$\frac{dA}{dt} = \oint \vec{v} \wedge \vec{\ell} = \oint v dl = -\frac{\lambda}{2\pi} \oint \kappa dl = -\lambda \left(1 - \frac{1}{2\pi} \sum_i \theta_i \right), \quad (12)$$

where θ_i are the turning angles of the tangent vector to the surface at the n possible vertexes or triple junctions between domains of different colour (we are now generalizing the discussion to models with multi-valued equilibrium states suchlike the Potts model with $q \geq 2$). In the Ising $q = 2$ model, $\sum_i \theta_i = 0$ since there are no such vertexes and we obtain $dA/dt = -\lambda$ for all hull-enclosed areas, irrespective of their size. If, instead, like in soap froths, there is a finite number of such vertexes with an angle of $2\pi/3$, that is, $\theta_i = \pi/3, \forall i$ (for highly anisotropic systems, as the Potts model, the angles are different from $2\pi/3$). The above equation thus reduces to the von Neumann law [28] for the hull-enclosed area A_n with a hull with n -turning angles:

$$\frac{dA_n}{dt} = \frac{\lambda}{6}(n - 6) \quad (13)$$

(in the Ising case $n = 0$). Whether a cell grows, shrinks or remains with constant area depends on its number of sides being, respectively, larger than, smaller than or equal to 6.

Conserved order parameter: bulk diffusion

A different type of dynamics occurs in the case of phase separation (a water and oil mixture ignoring hydrodynamic interactions or a binary alloy). In this case, the material is locally conserved, *i.e.* water does not transform into oil but they just separate. The main mechanism for the evolution is diffusion of material through the bulk of the opposite phase. After some discussion, it was established, as late as in the early 90s, that for scalar systems with conserved order parameter $z_d = 3$ (see [29, 8]).

Role of disorder: thermal activation

The situation becomes less clear when there is quenched disorder in the form of non-magnetic impurities in a magnetic sample, lattice dislocations, residual stress, *etc.* Qualitatively, the dynamics are expected to be slower than in the pure cases since disorder pins the interfaces. In general, based on an argument due to Larkin (and in different form to Imry-Ma) one expects that in $d < 4$ the late epochs and large scale evolution be no longer curvature driven but controlled by disorder.

The argument to estimate the growth law in dirty systems is the following. Take a system in one equilibrium state with a domain of linear size R of the opposite equilibrium state within it. This configuration could be the one of an excited state with respect to the fully ordered one with absolute minimum free-energy. Call $\Delta F(R)$ the free-energy barrier between the excited and equilibrium states. The thermal activation argument yields the activation time scale for the decay of the excited state (*i.e.* erasing the domain wall)

$$t_A \sim \tau_0 e^{\Delta F(R)/(k_B T)} . \quad (14)$$

For a barrier growing as a power of R , $\Delta F(R) \sim \Upsilon(T, J)R^\psi$ (where J represents the disorder) one inverts (14) to find the linear size of the domains still existing

at time t , that is to say, the growth law [30]

$$R(t) \sim \left(\frac{k_B T}{\Upsilon(T, J)} \ln \frac{t}{\tau_0} \right)^{1/\psi}. \quad (15)$$

All smaller fluctuation would have disappeared at t while typically one would find objects of this size. The exponent ψ is expected to depend on the dimensionality of space but not on temperature. In ‘normal’ systems ψ should be $d - 1$ – the surface of the domain. The pre-factor Υ is expected to be weakly temperature dependent.

To extend this result to the actual out of equilibrium coarsening situation one assumes that the same argument applies out of equilibrium to the re-conformations of a portion of any domain wall or interface where R is the observation scale.

However, not even for the (relatively easy) random ferromagnet there is consensus on the actual growth law [31]. We shall discuss a possible way out in Sect 5.1. In the case of spin-glasses, if the mean-field picture with a large number of equilibrium states were realized in finite dimensional models, the dynamics would be one in which all these states grow in competition. If, instead, the phenomenological droplet model applied, there would be two types of domains growing, $R(t) \sim (\ln t)^{1/\psi}$ and the dimension of the bulk of these domains should be compact but their surface should be rough with fractal dimension $d_s > d - 1$ [32].

4.2.2 Scaling functions

The scaling functions are harder to obtain. Indeed, there is no systematic method to derive them and all approximations dealt with are not accurate enough. For a much more detailed discussion of these methods see the review articles in [1]. Still, the super-universality property seems to be correct as we discuss in Sect. 5.2.

5 Dynamics of (weakly) random systems

In this Section I explain that the existence of a static typical length yields a natural crossover between the clean growth law, say $R \simeq [\lambda(T)t]^{1/2}$, and the activation-ruled one, $R \simeq [k_B T / \Upsilon \ln t]^{1/\psi}$, and how these two regimes might not be sufficiently separated in numerical and experimental measurements, being easily confused with a disorder and temperature dependent power [33].

I also discuss the super-universality hypothesis [32] and list some of its checks.

5.1 Crossover in the growing length

Numerical simulations of dirty systems tend to indicate that the growing

length is a power law with a disorder and T -dependent exponent. This can be due to the effect of a disorder and T -dependent cross-over length, as explained in [33]. For concreteness, let us assume that the width of the quenched random distribution is characterised by a parameter J and that the cross-over length depends on J/T . We call the latter L_T by absorbing the J dependence in T . The proposal is that below L_T the growth process is as in the clean limit while above L_T quenched disorder is felt and the dynamics are thermally activated above barriers that are usually taken to grow as a power of the size leading to eq. (15):

$$R(t) \sim \begin{cases} [\lambda(T)t]^{1/z_d} & \text{for } R(t) \ll L_T, \\ [k_B T/\Upsilon(T) \ln t]^{1/\psi} & \text{for } R(t) \gg L_T. \end{cases} \quad (16)$$

These growth-laws can be first inverted to get the time needed to grow a given length and then combined into a single expression that interpolates between the two regimes:

$$t(R) \sim e^{(R/L_T)^\psi} R^{z_d} \quad (17)$$

where the relevant T -dependent length-scale L_T has been introduced. Now, by simply setting $t(R) \sim R^{\bar{z}(T)}$ one finds

$$\bar{z}(T) - z_d \simeq z/L_T^\psi \quad \text{for times such that } t^{\psi/z_d} \ln t \simeq ct. \quad (18)$$

Similarly, by equating $t(R) \sim \exp(R^{\bar{\psi}(T)}/k_B T)$ one finds that $\bar{\psi}(T)$ is a decreasing function of T approaching ψ at high T .

5.2 Super-universality

In its first version the super-universality hypothesis states that in cases in which temperature and quenched disorder are ‘irrelevant’ in the sense that they do not modify the nature of the low-temperature phase (*e.g.* it remains ferromagnetic in the case of ferromagnetic Ising models with quenched random interactions) the scaling functions should not be modified [32]. Only the growing length changes from the, say, curvature driven $t^{1/2}$ law to an asymptotically slower law due to domain wall pinning by impurities. Tests of the disorder independence of the scaling functions of several correlations in quenches from $T > T_c$ into the ordered phase in the $3d$ RFIM [34] and the $2d$ RBIM [35, 36] (perhaps excluding the possibility of having zero bonds, see the discussion in Henkel & Pleimling) give support to this hypothesis.

We recently investigated two aspects of the super-universality hypothesis. On the one hand, we focused on the dependence on the initial condition of the space-time correlation scaling functions in the low temperature phase. With this aim, we studied the dynamics of the Potts model with different values of q after quenches from $T_0 \rightarrow \infty$ and $T_0 = T_c$ [25]. We found that the scaling functions are fully determined by the type of correlations present in the initial conditions

and basically of two types. All $2 \leq q \leq 4$ clean and weak disordered Potts models quenched from equilibrium at $T_0 \rightarrow \infty$ and clean $q > 4$ Potts models quenched from equilibrium at T_c (the transition is of first order) share their scaling function (see Fig. 6). Different functions are obtained after quenches from T_c in clean systems with $2 \leq q \leq 4$ and dirty systems with $q > 4$; in all these cases the transition is of second order and the critical exponents, in particular η , depend on q (although weakly) [37].

On the other hand, we analysed the geometric properties of areas and perimeters in the $2d$ RBIM and we discuss these results in the next section.

6 Statistics and geometry of coarsening

In [38, 22] we studied the distribution of domain areas, areas enclosed by domain boundaries, and perimeters for curvature-driven two-dimensional Ising-like coarsening, employing a combination of exact analysis and numerical studies, for various initial conditions. We showed that the number of hulls per unit area, $n_h(A, t) dA$, with enclosed area in the interval $(A, A + dA)$, is described, for a disordered initial condition, by the scaling function

$$n_h(A, t) = 2c_h / (A + \lambda_h t)^2, \quad (19)$$

where $c_h = 1/8\pi\sqrt{3} \approx 0.023$ is a universal constant and λ_h is a material parameter. For a critical initial condition, the same form is obtained, with the same λ_h but with c_h replaced by $c_h/2$. For the distribution of domain areas, we argued that the corresponding scaling function have the form

$$n_d(A, t) = (2)c_d(\lambda_d t)^{\tau-2} / (A + \lambda_d t)^\tau, \quad (20)$$

where c_d and λ_d are numerically very close to c_h and λ_h respectively, and the exponent τ is the one characterising the distribution of initial structures, critical percolation or critical Ising. These results were extended to describe the number density of the length of hulls and domain walls surrounding connected clusters of aligned spins. These predictions were supported by extensive numerical simulations. We also studied numerically the geometric properties of the boundaries and areas.

The derivation of eq. (19) is very easy. The number density of hull enclosed or domain areas at time t as a function of their initial distribution is

$$n(A, t) = \int_0^\infty dA_i \delta(A - A(t, A_i)) n(A_i, t_i) \quad (21)$$

with A_i the initial area and $n(A_i, t_i)$ their number distribution at the initial time t_i . $A(t, A_i)$ is the hull enclosed/domain area, at time t , having started from an area A_i at time t_i . The number density of hull-enclosed areas in critical

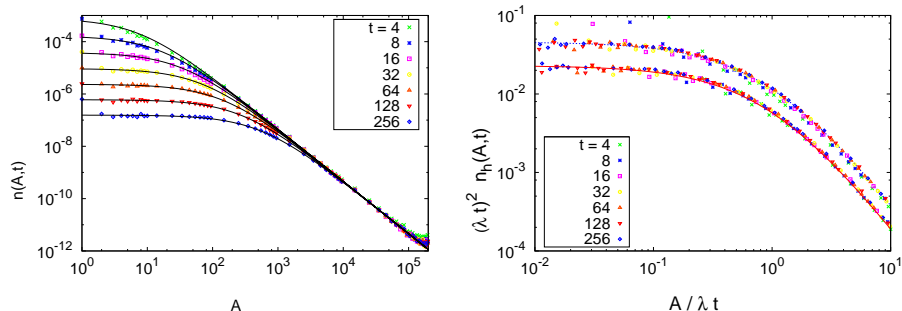


Figure 7: Left: number density of hull-enclosed areas at different times after a quench from $T_0 \rightarrow \infty$ to $T = 0$ in the $2dIM$; numerical results are shown with points and the analytic prediction with lines. There is only one fitting parameter, λ , that has been independently determined by a study of the space-time correlation. Right: comparison between the scaled number-density after a quench from $T_0 \rightarrow \infty$ (above) and $T_0 = T_c$ (below). Figure taken from [22].

percolation and critical Ising conditions was obtained by Cardy and Ziff [39]

$$n_h(A, 0) \sim \begin{cases} 2c_h/A^2, & \text{critical percolation,} \\ c_h/A^2, & \text{critical Ising.} \end{cases} \quad (22)$$

These results are valid for $A_0 \ll A \ll L^2$, with A_0 a microscopic area and L^2 the system size. Note also that we are taking an extra factor 2 arising from the fact that there are two types of hull enclosed areas, corresponding to the two phases, while the Cardy-Ziff result accounts only for clusters of occupied sites (and not clusters of unoccupied sites). $n_h(A, 0) dA$ is the number density of hulls per unit area with enclosed area in the interval $(A, A + dA)$ (we keep the notation to be used later and set $t = 0$). The adimensional constant c_h is a universal quantity that takes a very small value: $c_h = 1/(8\pi\sqrt{3}) \approx 0.022972$. The time dependent area is given by the Allen-Cahn result, $A(t) = A_i - \lambda_h(t - t_i)$. By simple integration of eq. (21) one obtains eq. (19).

It is interesting to note that the infinite temperature initial condition is not critical percolation on the square lattice. Still, it is very close to it an after coarse-graining $p = 1/2$ becomes critical continuous percolation. The dynamics of the discrete model, thus, very quickly settle into critical percolation ‘initial’ conditions and this determines the distribution of large structures dynamically. This observation was used by Barros *et al* to interpret freezing of $2d$ Ising models at very low temperatures [40].

The calculation of the number density of domain areas cannot be done analytically but a mean-field-like approximation that uses an expansion in powers

of c_h yields eq. (20), a result that is very convincing since it agrees well with numerical simulations [38, 22].

The discussion on the geometric properties of critical objects suggests to study the fractal properties of growing structures. In [38, 22] we pursued this line of research by analysing the relation between areas and perimeters during coarsening. We summarize the results below.

Several extensions of these results are: to the Ising model with conserved order parameter [41], the random bond Ising model [36], the Potts model [25], and coupled map lattices [42].

6.1 General picture

The summary of results in, and picture emerging from, the study of coarsening in $2d$ systems with Ising symmetry is the following.

(i) We *proved* scaling for the number density of hull-enclosed areas in bi-dimensional zero-temperature curvature-driven coarsening in the Ising universality class [38].

(ii) We argued that in these systems temperature effects are two-fold: they renormalize the pre-factor in the growth law and they introduce thermal domains that are distributed as in equilibrium. Their contribution to the total distribution of structures can be safely subtracted [22].

(iii) We obtained approximate expressions for the number density of domain areas and perimeters in curvature-driven coarsening in the $2d$ Ising universality class by using a mean-field-like analytic argument [22].

(iv) We checked results (i)-(iii) experimentally by analyzing the dynamics of a $2d$ liquid crystal [43].

(v) We derived the scaling functions of the number density of hull-enclosed areas, domain areas and perimeters for systems in the universality class of the $2d$ Ising model class with conserved order-parameter dynamics quenched from high-temperature by assuming that small structures behave roughly independently of each other [41].

(vi) We analysed the area number densities in the RBIM and we found that super-scaling holds once the growing length is modified to incorporate the slowing down due to pinning [36].

All these results are described by the following conjecture for the number density of domains and hull-enclosed areas [41]

$$R^{2\tau}(t) n_{d,h}(A, t) = \frac{(2)c_{d,h} \alpha^{2(\tau-2)} \left[\frac{A}{R^2(t)} \right]^{1/2}}{\left\{ 1 + \left[\frac{A}{R^2(t)} \right]^{z_d/2} \right\}^{(2\tau+1)/z_d}} \quad (23)$$

(this expression is exact for hull-enclosed areas in curvature-driven coarsening). z_d is the dynamic exponent (in the RBIM case, it is the effective temperature-

dependent one, \bar{z}_d). τ characterises the initial distribution. A way to derive eq. (23) is to assume that each time-dependent area is independently linked to its initial value by

$$A^{z_d/2}(t) \approx A_i^{z_d/2} - R(t), \quad (24)$$

In all these cases the expressions that we obtained have two distinct limiting regimes.

(vii) For areas that are much smaller than the characteristic area, $R^2(t)$, the distributions ‘feel’ the microscopic dynamics and thermal agitation while for areas that are much larger than $R^2(t)$ the distributions are simply those of the initial condition. For conserved order parameter dynamics the Lifshitz-Slyozov-Wagner [44] behaviour is recovered after a quench from $T_0 \rightarrow \infty$ and evolving at sufficiently low T . For critical Ising initial conditions the distribution of small areas does not approach the Lifshitz-Slyozov-Wagner. We conjectured that the reason is that our starting assumption, independence of domain wall motion for small domains, is not valid due to strong correlations in this case [41].

(viii) The distribution of the time-dependent areas that are larger than $R^2(t)$ are, in all cases, the ones of critical continuous percolation (for all initial conditions in equilibrium at $T_0 > T_c$) and critical Ising ($T_0 = T_c$).

We also studied the geometric properties and fractal dimensions of different objects during coarsening. We found that

(ix) Small structures are compact and tend to have smooth boundaries, that are pretty close to circular ($A \sim p^2$) in the conserved order-parameter case and a little bit less so for non-conserved order-parameter dynamics.

(x) The long interfaces retain the fractal geometry imposed by the equilibrium initial condition.

In [43] we performed experiments in a $2d$ liquid crystal that evolves through the formation of domains of two chiralities. The analysis of data confirmed that the dynamics is of curvature-driven type, in the sense that the correlation functions scale with $R \sim t^{1/2}$ and, moreover, after a careful analysis of noise originated in the data acquisition procedure, we obtained a hull-enclosed area distribution function that agrees well with the theoretical prediction.

The geometrical analysis of coarsening cells in the $2d$ Potts model will be presented in [25]. One might expect that other dynamic systems, once in the Ising non-conserved order parameter universality class, such as some voter models [10], should have similar area distributions. The case of a $2d$ Edwards-Anderson model has not been analyzed yet.

As future work we plan to investigate how these results extend to $3d$ systems by analyzing volume distributions as well as area distributions on $2d$ cuts. Three dimensional phase separation of a binary mixture is realized by different physical systems, in particular the one studied in [45], that promises to be a nice material where to confront the results of analytics and simulations to experiments.

7 Coarsening in the spiral model

Among other features, in [15] we studied the dynamics of the spiral model after a sudden quench, in which a completely empty configuration is evolved from time $t = 0$ onwards with the dynamic rule specified by a different value of $p > p_0$. This procedure is similar to the temperature quench of a liquid. For $p < p_c$, after a non equilibrium transient the system attains a non-blocked equilibrium state. The relaxation time for attaining such a state diverges as $p \rightarrow p_c$. In the critical case with $p = p_c$, the system approaches the blocked equilibrium state by means of an aging dynamics similar to that observed in critical quenches of ferromagnetic models. Freezing is not observed because the dynamic density $\rho(t)$ is always smaller than the critical one $\rho_c = p_c$, at any finite time. Something different happens for filling at $p > p_c$. The system keeps evolving but a blocked state is never observed despite the fact that the density of particles exceeds $\rho_c = p_c$ at long enough times. This is no surprise since the dynamics are fully reversible: for any p , each configuration reached dynamically can always evolve back to the initial empty state by the time reversed process, although with a very low probability. Therefore, a blocked state cannot be dynamically connected to the initial empty state. The dynamics of the spiral model at $p > p_c$ strongly resembles coarsening in ferromagnets, as illustrated in the centre and right panels in Fig. 2. In the $p \simeq 1$ limit in which the dynamics can be analyzed semi-analytically the system coarsens by forming longer and longer one-dimensional objects of vacancies that are almost frozen but not completely since they could be destroyed by the boundaries. The density of these objects is irrelevant in the large size limit and the density of particles can asymptotically approach 1 although the system is never blocked.

Acknowledgments I wish to thank J. J. Arenzon, C. Aron, M. Baity-Jesi, G. Biroli, A. J. Bray, S. Bustingorry, C. Chamon, F. Corberi, A. Jelic, J. L. Iguain, A. B. Kolton, M. P. Loureiro, M. Picco, Y. Sarrazin and A. Sicilia for our collaboration on phase ordering problems that lead to the new results discussed in these notes. I also wish to thank E. Domany, P. Krapivsky, D. Vandembroucq, and F. Vázquez for recent discussions on this problem.

References

- [1] A. J. Bray, Adv. Phys. **43**, 357 (1994). P. Sollich, *Introduction to phase ordering kinetics*, <http://www.mth.kcl.ac.uk/~psollich/> *Kinetics of phase transitions*. S. Puri and V. Wadhawan, eds. (CRC Press, Taylor & Francis).
- [2] D. Stauffer and A. Aharony, *Introduction to percolation theory* 2nd edition,

- (Taylor & Francis, 2003). W. Werner, *Lectures on two dimensional critical percolation*, arXiv:0710.0856 G. R. Grimmet, *Percolation* 2nd edition (Springer, 1999).
- [3] H. Hinrichsen, *Adv. Phys.* **49**, 815 (2000).
 - [4] For a historical survey see B. Berche, M. Henkel, and R. Kenna, *Critical phenomena: 150 years since Cagniard de la Tour*, arXiv:0905.1886. N. Goldenfeld, *Lectures on Phase Transitions and the Renormalization Group* (Addison Wesley, 1991).
 - [5] F. Y. Wu, *Rev. Mod. Phys.* **54**, 235 (1982).
 - [6] J. Stavans, *Rep. Prog. Phys.* **56**, 733 (1993).
 - [7] see, *e.g.* H. Risken *The Fokker-Planck equation: methods of solution and applications* (Springer, 1989). C. Gardiner, *Handbook Of Stochastic Methods: For Physics, Chemistry And The Natural Sciences* (Springer Series In Synergetics).
 - [8] G. Barkema and M. E. J. Newman, *Monte Carlo methods in statistical physics* (Clarendon Press, 2001).
 - [9] J. Miller and D. Huse, *Phys. Rev. E* **48**, 2528 (1993).
 - [10] See, *e.g.* F. Vázquez and C. López, *Phys. Rev. E* **78**, 061127 (2008) O. Al Hammal, H. Chaté, I. Dornic, and M. A. Muñoz *Phys. Rev. Lett.* **94**, 230601 (2005).
 - [11] J. Jäckle, *J. Phys. Cond. Matt.* **14**, 1423 (2002). P. Sollich and F. Ritort, *Adv. in Phys.* **52**, 219 (2003). S. Leonard, P. Mayer, P. Sollich, L. Berthier, and J. P. Garrahan, *J. Stat. Mech.* P07017 (2007).
 - [12] C. Toninelli, G. Biroli, and D. S. Fisher, *Phys. Rev. Lett.* **96** 035702 (2006).
 - [13] J. Reiter, F. Mauch, and J. Jäckle, *Physica A* **184**, 458 (1992). S. J. Pitts, T. Young, and H. C. Andersen, *J. Chem. Phys.* **113**, 8671 (2000). M. Sellitto, G. Biroli, and C. Toninelli, *Europhys. Lett.* **69**, 496 (2005).
 - [14] G. Biroli and C. Toninelli, *Eur. Phys. J. B* **64**, 567 (2008). C. Toninelli and G. Biroli, *J. Stat. Phys.* **130**, 83-112 (2008). C. Toninelli, G. Biroli, and D. S. Fisher, *Phys. Rev. Lett.* **98** 129602 (2008).
 - [15] F. Corberi and L. F. Cugliandolo, *J. Stat. Mech.* (2009).
 - [16] C. M. Fortuin and P. W. Kasteleyn, *Physica* **57**, 536 (1972).
 - [17] B. Duplantier, *Conformal Fractal Geometry and Boundary Quantum Gravity* arXiv:math-ph/0303034.

- [18] C. Vanderzande and A. L. Stella, *J. Phys. A* **22**, L445 (1989).
- [19] W. Janke and A. M. J. Schaakel, *Nucl. Phys. B* **700** [FS] 385 (2004).
- [20] M. Picco, R. Santachiara, and A. Sicilia, *J. Stat. Mech.* P04013 (2009).
- [21] H. Saleur and B. Duplantier, *Phys. Rev. Lett.* **58**, 2325 (1987).
- [22] A. Sicilia, J. J. Arenzon, A. J. Bray, and L. F. Cugliandolo, *Phys. Rev. E* **76**, 061116 (2007).
- [23] B. Schmittmann, R. K. P. Zia, in *Phase transitions and critical phenomena*, vol. 17, ed by C. Domb and J. L. Lebowith (Academic Press, NY, 1995). U. C. *Field-theory approaches to nonequilibrium dynamics* in Summer School on Ageing and the Glass Transition, Lecture notes in physics **716**, 295 (2007). A. Gambassi and P. Calabrese, *J. Phys. A* **38**, R133 (2005).
- [24] H. K. Janssen, B. Schaub, B. Schmittmann, *Z. Phys. B* **73**, 539 (1989).
- [25] M. P. Loureiro, J. J. Arenzon, A. Sicilia, and L. F. Cugliandolo, in preparation.
- [26] S. M. Allen and J. W. Cahn, *Acta Metall.* **27**, 1085 (1979).
- [27] D. Kandel and E. Domany, *J. Stat. Phys.* **58**, 685 (1990). L. Chayes, R. H. Schonmann, and G. Swindle, *J. Stat. Phys.* **79**, 821 (1995).
- [28] J. von Neumann, in *Metal interfaces*, ed. C. Herring (American Society for Metals, 1952), p. 108-110.
- [29] D. A. Huse, *Phys. Rev. B* **34**, 7845 (1986).
- [30] D. A. Huse and C. L. Henley, *Phys. Rev. Lett.* **54**, 2708 (2004).
- [31] see, *e.g.* H. Rieger, G. Schehr, and R. Paul, *Prog. Theor. Phys. Suppl.* **157**, 111 (2005) and references therein.
- [32] D. S. Fisher and D. A. Huse, *Phys. Rev. B* **38**, 373 (1988).
- [33] J. L. Iguain, S. Bustingorry, A. B. Kolton, and L. F. Cugliandolo, *Phys. Rev. B* **80**, 094201 (2009).
- [34] M. Rao and A. Chakrabarti, *Phys. Rev. Lett.* **71**, 3501 (1993). C. Aron, C. Chamon, L. F. Cugliandolo, and M. Picco, *J. Stat. Mech.* P05016 (2008).
- [35] S. Puri and N. Parekh, *J. Phys. A* **26**, 2777 (1993). A. J. Bray and K. Humayun, *J. Phys. A* **24**, L1185 (1991). M. Henkel and M. Pleimling, *Phys. Rev. B* **78**, 224419 (2008).

- [36] A. Sicilia, J. J. Arenzon, A. J. Bray and L. F. Cugliandolo, EPL **82**, 10001 (2008).
- [37] J. L. Jacobsen and M. Picco, Phys. Rev. E **61**, R13 (2000).
- [38] J. J. Arenzon, A. J. Bray, L. F. Cugliandolo, and A. Sicilia, Phys. Rev. Lett. **98**, 145701 (2007).
- [39] J. Cardy and R. Ziff, J. Stat. Phys. **110**, 1 (2003).
- [40] K. Barros, P. L. Krapivsky and S. Redner, arXiv:0905.3521, submitted to Phys. Rev. Lett.
- [41] A. Sicilia, Y. Sarrazin, J. J. Arenzon, A. J. Bray, and L. F. Cugliandolo, Phys. Rev. E **80**, 031121 (2009).
- [42] A. Sicilia, L. F. Cugliandolo, and E. Katzav, in preparation.
- [43] A. Sicilia, J. J. Arenzon, I. Dierking, A. J. Bray, L. F. Cugliandolo, J. Martinez-Perdiguero, I. Alonso, and I. C. Pintre, Phys. Rev. Lett. **101**, 197801 (2008).
- [44] I. M. Lifshitz and V. V. Slyozov, J. Phys. Chem. Solids **19**, 35 (1961). C. Wagner, Z. Elektrochem. **65**, 581 (1961).
- [45] D. Dalmas, A. Lelarge, and D. Vandembroucq, Phys. Rev. Lett. **101**, 255501 (2008).